Sensitivity Optimization of Printed Spiral Coil for Wireless Resistive Analog Passive (WRAP) Sensors using Genetic Algorithm*

Babak Noroozi, *Student Member, IEEE*, and Bashir I. Morshed, *Member, IEEE, EMBS*

***Abstract*— Body-worn battery-less Wireless Resistive Analog Passive (WRAP) sensor can be unobtrusive while collecting physiological data continuously. Inductive connection between a pair of Printed Spiral Coils (PSC) eliminates the intrusive wires. Inductive connection of primary and secondary PSC enabled us to probe the body signals using the inductive link. The primary side voltage is modulated by the sensed body signal at the secondary PSC. The coil physical characteristics influence the sensitivity which is defined as observed voltage changes over the sensor variation. We have previously reported an iterative method to optimize the coil specifications for maximum sensitivity with constrained coil profile size by maximizing the power transfer efficiency from primary to secondary. In this study sensitivity is maximized by first, driving an analytical multivariable equation of circuit components and physical characteristics, and then using Genetic Algorithm (GA) to maximize it with considering the size and fabrication constraints. The results are compared to the other methods that shows a higher result in the range of 10^2 comparing to the best alternate methods (sqp). It helps us to detect smaller physiological signals in the noisy environment.**

I. Introduction

Wireless connection between a pair of magnetic coils has recently drawn a tremendous research attention for various applications, especially for the power transfer of high power electric vehicle [1], [2], [3] and low power implantable medical devices [4], [5]. Their major concern is focused on maximizing the efficiency of transferred power as well as minimizing the impact of distance and misalignment between primary and secondary coils [6], [7].

We suggested a new wireless resistive analog passive (WRAP) sensors that employs the inductive connection between two planar printed spiral coils (PSC) to sense the body signals with a resistive sensor and modulate the primary coil amplitude of carrier signal [8]. The suggested method makes the wearable sensors more practical both in technical and economical perspectives. Small, low-price, and sensitive coils make them clinically feasible but these factors do not increase simultaneously: increasing the sensitivity increases the size and consequently the cost of sensors. Therefore, we design a pair of coils that has maximum output voltage variation over the sensor resistance changes, with considering the size and fabrications constraints. Previously, we have reported the results of coil design with an iterative optimization method targeted the power transfer efficiency [8]. In this paper, the closed form of sensitivity is derived and optimized using Genetic Algorithm (GA) and convex optimization methods and the all the results are compared for the highest sensitivity.

*This material is based upon work supported by the National Science Foundation under Grant No. 1637250.

B. Noroozi and B. I. Morshed are with the department of Electrical and Computer Engineering (EECE), The University of Memphis, Memphis, TN 38152, USA. (Corresponding author Email: bnoroozi@memphis.edu)

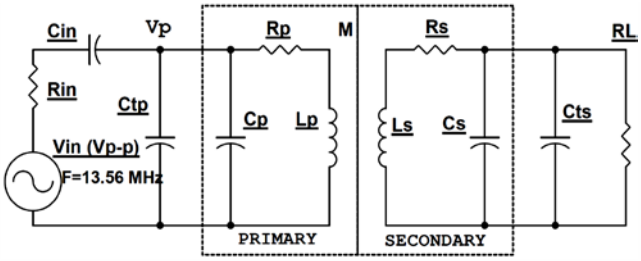

Figure 1. Circuit diagram of primary and secondary and their tuning capacitors. R_L is the transducer resistor. Here R_{in}=50 Ω, C_{in}=3.35 µF, Ctp=50 pF (tuning, secondary), k=0.07 ($M = k\sqrt{L_P L_S}$), Cts=138 pF (tuning primary).

II. Circuit Model

Fig. 1 shows the schematic of the simplified equivalent primary (scanner) and secondary (sensor) circuits. The dashed line encompasses the primary and secondary equivalent circuits of the PSCs. Inductive link connects the passive secondary circuit to the primary side which is tuned on 13.56 MHz, within the ISM (Industrial, Scientific, Medical) Radio frequency bands. A resistive transducer (R_L) models the probing (body) signals as resistance variation. This body signal variation reflects to the primary voltage, Vp, through the inductive link (M). Sensitivity is defined as the change of V_P over the unit change in R_L (1).

$$Sensitivity = \Delta V_P/\Delta R_L = dV_P/dR_L \quad (1)$$

Fig. 2 depicts the planar coil physical specifications and characteristics with relation to the coils equivalent components as defined in section III. In Fig. 1, R_{in} and C_{in} are the signal generator equivalent internal resistor and capacitor and C_{tp} is tuning capacitor to tune the primary resonance frequency to 13.56 MHz. In the secondary circuit, C_{ts} and R_L are the tuning capacitor and resistive transducer, respectively. Primary and secondary coils are inductively coupled with mutual inductance M that is defined by primary, secondary, and the coupling factor, k, as shown in (2).

$$M = k\sqrt{L_P L_S} \quad (2)$$

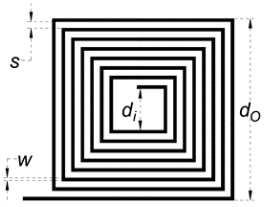

Figure 2. Planar Spiral Coil (PSC) physical specifications.

III. Circuit Analysis and Equations

In this section, the sensitivity closed form equation as a function of circuit components and coil physical characteristics is derived. Fig. 2 is redrawn in Fig. 3 that shows the equivalent impedance of the secondary side (Z_2) and its reflection to the primary side (Z_R). It can be shown that:

$$Z_R = -M^2/Z_2 \tag{3}$$

$$Z_2 = R_S + j\omega L_S + R_L/(1 + j\omega R_L C_2) = \left[R_S + \frac{R_L}{1+(R_L C_S \omega)^2} + j\omega\left(L_S - \frac{C_S {R_L}^2}{1+(R_L C_S \omega)^2}\right)\right] \tag{4}$$

$$V_P = \frac{1}{1+\left(R_{in}+\frac{1}{j\omega C_{in}}\right)\times\left(j\omega C_1+\frac{1}{R_P+j\omega L_P+Z_R}\right)} \times V_{in} \tag{5}$$

Where: $C_1 = C_p + C_{tp}$ and $C_2 = C_S + C_{ts}$.

Equations (6) to (12) show the coil equivalent components as the function of coil physical characteristics [8].

$$L = \frac{1.27 n^2 \mu_0 (d_o + d_i)}{4}\left[ln\left(\frac{2.07}{\varphi}\right) + 0.18\varphi + 0.13\varphi^2\right] \tag{6}$$

$$R_S = \rho\frac{l_c}{w} \times \frac{1}{\delta.(1-\exp(-t_c/\delta))} \text{ (series resistor with L)} \tag{7}$$

$$\delta = \sqrt{\rho/\pi\mu f} \tag{8}$$

Conductor length:

$$l_C = 4nd_O - 3nw - (2n-1)^2(s+w) \tag{9}$$

$$C_P = C_{PC} + C_{PS} \approx (\alpha\varepsilon_{rc} + \beta\varepsilon_{rs})\varepsilon_0 \frac{t_C}{s} l_g \tag{10}$$

$$L_g = 4(d_O - nw)(n-1) - 4n(n+1)s \text{ (Gap length)} \tag{11}$$

φ, "Fill-Factor", is defined as:

$$\varphi = (d_O - d_i)/(d_O + d_i) \tag{12}$$

Since the sensitivity is defined as the amplitude change of output voltage, the magnitude of output voltage and its derivative are of interest. Then, by normalizing and taking derivative of (5), the final sensitivity objective function can be found as (13):

$$Sensitivity(d_{O1}, n_1, s_1, w_1, n_2, s_2, w_2, R_L) = -|d(|V_P/V_{in}|)/dR_L| \tag{13}$$

Where $d_{Oi}, n_i, s_i,$ and w_i are the coil outer size, number of turns, space between tracks, and the width of the tracks for the primary (i=1) and secondary (i=2) coils, respectively. Because the optimization algorithms look for minimum value of the objective function we consider the negative of absolute value to search for the best (highest) sensitivity. The secondary coil size is fixed at 20 mm as a constraint, then sensitivity in (13) is a function of eight variables, coil physical characteristics, as well as sensor resistance (R_L). C_{in} and R_{in} are defined by the signal generator, and the primary and secondary tuning capacitors, C_{pt} and C_{st}, are defined as previous results of iterative method [8]. Then, (13) is the multivariable equation that the optimization algorithm(s) will minimize it.

TABLE I. Variables Lower and Upper Bounds

Variables	d_{O1} (mm)	n_1	s_1 (mil)	w_1 (mil)	n_2	s_2 (mil)	w_2 (mil)	R_L (KΩ)
Lower Bound	20	5	6	20	5	6	6	1
Upper Bound	50	20	70	70	20	70	70	1.5

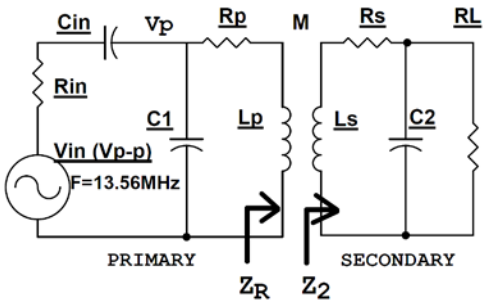

Figure 3. Secondary equivalent impedance and the reflected impedance from secondary to the primary. $C_1 = C_p + C_{tp}$ and $C_2 = C_S + C_{ts}$

IV. Optimization

A. Constraint and bounds

Linear and non-linear constraints and bounds are common in all optimization methods. The coils have the highest share in the primary and secondary circuits, then the primary and secondary circuit sizes are almost the same as the size of coils. To keep the secondary coil small and practically applicable, it is fixed at the d_{O2}=20 mm, while the primary coil is confined to $(d_{O2})_{max}$=40 mm. The minimum space between tracks and the width of the tracks on the PCB are confined by the fabrication foundry (Oshpark) to 6 mil (=6×25.4×10^{-3} mm). As there is no restriction for the number of turns, number of primary and secondary coil turns are set arbitrary. The upper and lower bounds of variables are listed in Table I. Since the transducer resistance that we utilize are in the range of 1 kΩ, its bound are considered accordingly.

Regarding Fig. 2, the inner size of a coil is determined by d_O, n, s, and w that makes the two nonlinear constraints for primary and secondary coils, as they cannot be less than zero. Then, non-linear constraints are:

$$d_{ij} = d_{oj} - [2n_j w_j + 2(n_j - 1)s_j] \geq 0 \tag{14}$$

Where j=1, 2 for the primary and secondary, respectively, and d_i is the inner size of the coil (Fig. 2).

B. Optimization algorithms

Because of the complicated form of multivariable objective function (13), optimization algorithm is more likely to find a local minimum. Therefore, we apply both analytic and stochastic optimization methods and the results are evaluated from the behavior of objective function at, and around the optimum point.

Three algorithms: “interior-point”, “sqp”, and “active-set” have been utilized as the classic optimization methods for comparison. A typical classic algorithm generates a single point and through an iterative deterministic computation tries to approach to the optimum point, while Genetic Algorithm (GA) as a stochastic technique, generates a broad random population and by using different methods of mutation, crossover, scaling and selection, finds the next generation to converge to the optimum point. Since GA is a nondeterministic algorithm, different runs may end to the different results but choosing the appropriate settings and options makes it more likely to reach to the almost identical results. Table II shows GA relevant options and settings. To find the best crossover fraction, the fitness values were calculated for crossover fraction swept from 0 to 1 and the best value (0.3) was selected.

V. Results

Fig. 4 shows the sensitivity plots using the “sqp” algorithm around the optimum point which is represented by dots in this figure. As it can be seen, the optimization result is not even a local minimum which might be due to the non-convexity and high non-linearity of the objective function. For the two other classic algorithms, “active-set” and “interior-point”, the results are not local minima as well.

Fig. 5 shows the sensitivity plots around the optimum point for Genetic Algorithm (GA), and it can be seen that the GA has truly found the minimum point. For the setting shown in Table II, GA was run thirty times and the minimum, mean, and standard deviation of sensitivity were -1.1×10^{-3}, -0.95×10^{-3}, and 0.17×10^{-3}, respectively. Fig. 6 illustrates how GA convergences to the optimum point. Table III shows the results of different algorithms along with previously reported iterative method [8]. The results represent that GA found the global optimum value within the constraints as well as the highest sensitivity which is almost two order higher than the best result of the other methods (sqp).

VI. Conclusion

Optimizing the printed spiral coils (PSC) in order to find the maximum sensitivity of overall system with minimum coil size is an important factor to make the wireless resistive analog passive (WRAP) sensors. We previously optimized the coil design based on the iterative method that used the power transfer efficiency formulation. In this paper, we first formulized the sensitivity as a multivariable function of primary and secondary coil physical characteristics and sensor resistance. Then considering the size and manufacturing constraints, the coils were optimized with three deterministic methods (interior-point, active-set, sqp) and one stochastic method, Genetic Algorithm. The results are compared with our previously reported iterative method.

After several trials and exploring the best options and settings, GA reached to the global highest sensitivity that is two order higher than the best results (sqp) of the other methods. It helps us to probe the smaller physiological signals

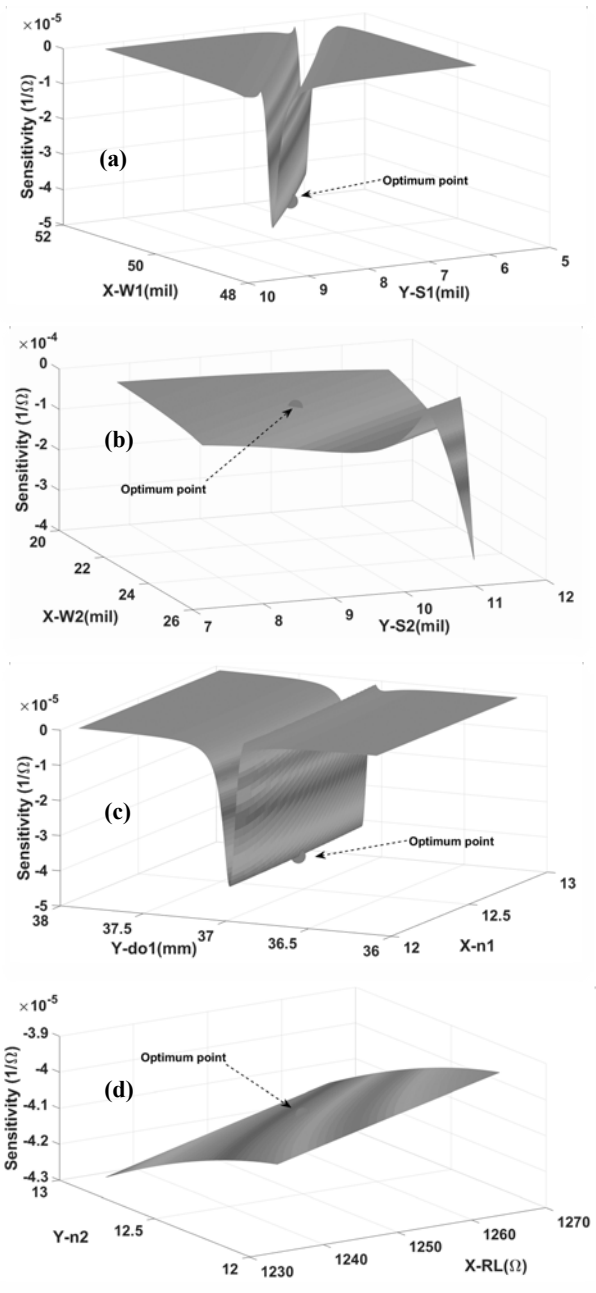

Fig. 4. “sqp” optimization results, sensitivity vs different variables. In each plot, two variables are changed around the optimum point, while the other six variables are the optimum point coordinates. For (b) and (d) the optimum point is a true minimum, but not for other cases.

TABLE II. Relevant GA options used in this study

Maximum generation	200
Population size	3000
Crossover Fraction	0.3
Crossover Function	Scattered
Mutation Function	Adaptive Feasible (for non-linear constraints
Non-linear Constraint algorithm	Penalty
Fitness scaling	Rank
Selection Function	Stochastic uniform
Elite count	150 (5% of population)

in the noisy environment of body. Although it might even improve with further fine tuning to achieve the absolute highest sensitivity, but because of PSC fabrication process variability and tolerance, practical results will be limited by the actual coil physical dimensions. Future work will investigate the effect of fabrication tolerance on the sensitivity and attempt to minimize the gradient of sensitivity to all the variabilities of this multi-objective optimization.

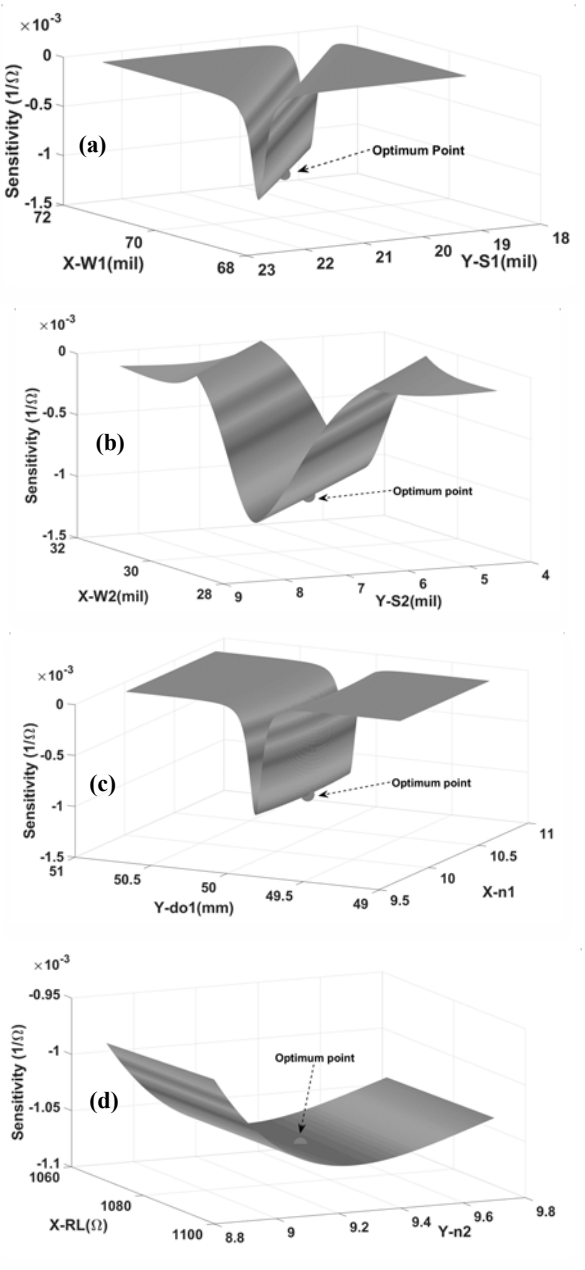

Fig. 5. GA optimization results, sensitivity vs different variables. In each plot two variables are changed around the optimum point, while the other six variables are the optimum point coordinates. The optimum point is a true minimum in all plots.

TABLE III. OPTIMIZED VALUES FOR DIFFERENT ALGORITHMS DEPICTING THAT GENETIC ALGORITHM LEADS TO THE HIGHEST SENSITIVITY.

Algorithm	Optimal values of the Variables								Sensitivity (1/ Ω)
	d_{O1} (mm)	n_1	s_1 (mil)	w_1 (mil)	n_2	s_2 (mil)	w_2 (mil)	R_L (KΩ)	
Iterative method	40	9	20	50	9	6	31	1	3×10^{-7}
Interior point	44.4	8	12.3	57.8	7.5	11.4	25.5	1.25	1.8×10^{-5}
Active set	34.5	12.5	6	46.1	12.5	12.6	19.9	1.25	3.75×10^{-5}
sqp	37	12.5	7.6	50.2	12.5	9.5	22.8	1.25	4×10^{-5}
Genetic Algorithm	47.2	10.1	16.8	66.3	9.2	6.4	30	1.15	1.1×10^{-3}

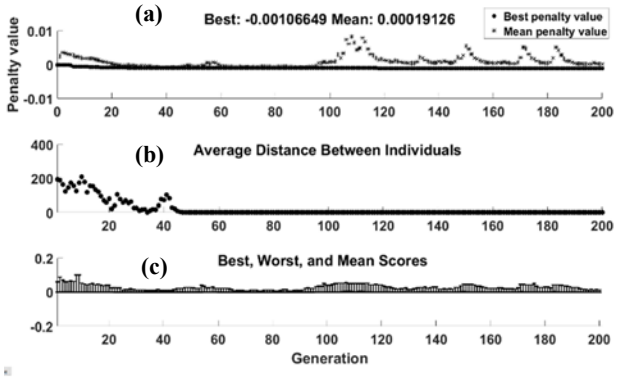

Fig. 6. The convergence of GA. (a) Penalty value for non-linear constraint algorithm. (b), (c) Decreasing the average distance between individuals and the diversity indicate the convergence of algorithm.

REFERENCES

[1] F. Liu, Y. Yang, D. Jiang, X. Ruan, and X. Chen, "Modeling and Optimization of Magnetically Coupled Resonant Wire less Power Transfer System With Varying Spatial Scales," *IEEE Trans. on Power Electronics*, vol. 32, no. 4, pp. 3240-3250, 2017.

[2] C. Qiu, K. T. Chau, C. Liu, W. Li, and F. Lin, "Quantitative comparison of dynamic flux distribution of magnetic couplers for roadway electric vehicle wireless charging system," *J. Appl. Phys.,* vol. 115, no. 17, pp. 17A334-1–17A334-3, May 2014.

[3] J. D. Heebl, E. M. Thomas, R. P. Penno, and A. Grbic, "Comprehensive analysis and measurement of frequency-tuned and impedance-tuned wireless non-radiative power-transfer systems," *Antennas and Propagation Magazine, IEEE*, vol. 56, no. 5, pp. 131–148, Oct 2014.

[4] Y. M. Roshan and E. J. Park, "Design approach for a wireless power transfer system for wristband wearable devices," *IET Power Electronics*, vol. 10, no. 8, pp. 931-937, 6 30 2017.

[5] Z. Chen, H. Sun, and W. Geyi, "Maximum Wireless Power Transfer to the Implantable Device in the Radiative Near Field," *IEEE Antennas and Wireless Propagation Letters,* vol. 16, pp. 1780-1783, March 2017.

[6] S. Raju, R. Wu, M. Chan, and P. Yue, "Modeling of Mutual Coupling Between Planar Inductors in Wireless Power Applications, " *IEEE Trans. On Power Electronics*, vol. 29, no. 1, pp. 481-490, Jan. 2014.

[7] S. I. Babic, F. Sirois, and C. Akyel, "Validity check of mutual inductance formulas for circular filaments with lateral and angular misalignments," *Progress In Electromagnetics Research M,* vol. 8, pp. 15-26, 2009.

[8] B. Noroozi and B. I. Morshed, "PSC Optimization of 13.56-MHz Resistive Wireless Analog Passive Sensors," in *IEEE Trans. on Microwave Theory and Techniques*, vol. 65, no. 9, pp. 3548-3555, Sept. 2017.